Physics of the Solid State, Vol. 43, No. 3, 2001, pp. 556–562. Translated from Fizika Tverdogo Tela, Vol. 43, No. 3, 2001, pp. 536–542.

LOW-DIMENSIONAL SYSTEMS AND SURFACE PHYSICS

Fluctuational Dissipative Electromagnetic Interaction between a Nanoprobe and a Surface

G. V. Dedkov and A. A. Kyasov

Kabardino-Balkar State University, Nalchik, 360004 Russia
e-mail: gv_dedkov@rekt.kbsu.ru

Received May 30, 2000

Abstract—In the framework of fluctuational electromagnetic theory, analytical expressions are obtained for the dynamic dissipative damping forces acting on the probe of an atomic-force microscope (AFM), as well as between two plane surfaces at their contact. The contacts between materials typical of AFM, quartz-microbalance, and surface-force apparatus experiments are considered. The conditions for nondissipative slide are discussed. A comparison between the calculated oscillator quality factor associated with fluctuational dissipative forces and its values obtained in AFM experiments with a silicon probe and a mica sample shows that they are of the same order of magnitude; therefore, an experimental investigation of such forces is feasible. © *2001 MAIK "Nauka/Interperiodica".*

INTRODUCTION

Nanostructural mechanisms of energy dissipation play a decisive role in the problem of friction as a whole, and the fluctuational dissipative electromagnetic interaction is one of the most important factors in the process of contactless slide of surfaces [1]. This process is typical of the dynamical mode of operation of an atomic-force microscope (AFM), and, therefore, experimental AFM studies of dissipative forces have considerable promise [2, 3].

In our recent papers [4, 5], the problem of damping of atomic and molecular particles moving laterally over the surface of a solid at a nonrelativistic velocity V was treated in detail in the framework of the general theory of fluctuational electromagnetic interactions. The objective of this paper is further development and application of this theory for calculating dissipative forces acting on an AFM probe in the cases of different combinations of the materials of the probe and sample. We also discuss the role of fluctuational electromagnetic forces in measurements with a quartz microbalance [6, 7] and treat the problem on the friction of two plane surfaces, which is the subject of some controversy in the literature [8–10].

1. DAMPING FORCE ON ATOMIC AND MOLECULAR PARTICLES: THE PRINCIPAL THEORETICAL RESULTS

The physical processes resulting in fluctuational dissipative interactions are similar to those that lead to conservative van der Waals attractive forces between solids. The latter forces are due to quantum-mechanical and thermal fluctuations of microscopic electric fields associated with motion of charged particles. These fluctuating fields induce analogous fields in other interacting solids, and, when the solids move relative to each other, the interaction between them is accompanied by Joule loss, which is considered the result of dynamical damping.

In order to strictly calculate the fluctuational dissipative interaction force between an arbitrarily shaped nanoprobe and a plane (or curved) surface in the framework of the theory developed in [4, 5], one should determine the equilibrium fluctuation spectrum of the electromagnetic field in the gap between the solids, which is a complicated mathematical problem in itself. In this case, some geometrical restrictions arise which reflect the fundamental properties of forces of this kind, in particular, of conservative van der Waals forces. In the latter case, fortunately, the assumption of additive interactions between individual particles is a close approximation, which allows one to correctly calculate the dependence of the resultant forces upon the spacing between the solids; only the interaction constant is affected by this approximation [11]. For a convex probe and a plane surface, this constant, as calculated in the additive-interaction approximation, is more than 5–20% in error and can be corrected by its effective renormalization [12].

As a working hypothesis, we assume that the fluctuational dissipative forces are also additive and that this additivity approximation gives the correct distance dependence of the forces. A comparison with calculations that do not involve this approximation is further shown (Section 5) to provide support for this assumption.

Following [4, 5], we consider the case where an atom (molecule) moves at a nonrelativistic velocity V parallel to the surface of a medium with a dielectric function $\varepsilon(\omega)$ and is at a distance h from the surface. A

neutral spherical particle is characterized by polarizability $\alpha(\omega)$, while a dipole molecule is assumed to have an arbitrarily oriented constant dipole moment **d**.

In the limit of small velocities (which is of prime interest for the dynamical mode of the AFM operation, in which the typical nanoprobe velocities do not exceed or are much smaller than 1 m/s) and in the range of distances $r_0 \ll h \ll c/\omega_0$ (where r_0 is the characteristic size of atoms and ω_0 is the frequency of orbital motion of electrons), the damping force per atom was found to be [4, 5]

$$F = -\frac{3\hbar V}{8\pi h^5}\int_0^\infty d\omega\left\{2\left[\alpha''(\omega)\frac{d\Delta''(\omega)}{d\omega} - \Delta''(\omega)\frac{d\alpha''(\omega)}{d\omega}\right]\right. \quad (1)$$
$$\left. + \omega\left[\alpha''(\omega)\frac{d^2\Delta''(\omega)}{d\omega^2} - \Delta''(\omega)\frac{d^2\alpha''(\omega)}{d\omega^2}\right]\right\}\coth\left(\frac{\omega\hbar}{2k_BT}\right),$$

where $\Delta(\omega) = (\varepsilon(\omega) - 1)/(\varepsilon(\omega) + 1)$ and the doubly primed quantities are the imaginary parts of the corresponding functions. At $T = 0$, after some mathematical manipulation, Eq. (1) is reduced to a simpler formula:

$$F = -\frac{3\hbar V}{4\pi h^5}\int_0^\infty d\omega\alpha''(\omega)\frac{d\Delta''(\omega)}{d\omega}. \quad (2)$$

We note that the condition $r_0 \ll h \ll c/\omega_0$ allows one to treat the particle as a point dipole and ignore the retardation effects. In this case, the distance to the surface is limited from above by a value of 10–20 nm, which is the exact value at which probing is efficiently performed in the dynamical mode of the AFM operation. At $h \approx r_0$, spatial dispersion effects become significant and the dependence of the dielectric function upon the wave vector should be taken into account. Nonetheless, in this case, too, Eqs. (1) and (2) account for a certain (perhaps, dominant) part of the interaction. Here, the situation is analogous to that which takes place when one calculates the interaction energy between two neutral atoms in the vicinity of the van der Waals minimum: the dipole–dipole interaction makes a significant contribution to the interatomic interaction energy, although, strictly speaking, the atoms cannot be considered as point dipoles when the separation between them is so small.

Damping of motion of a dipole molecule with dipole moment $\mathbf{d} = (d_x, d_y, d_z)$ is characterized by the dissipative force [5]

$$F = -\frac{3(3d_x^2 + d_y^2 + 4d_z^2)V}{32\sigma h^5}, \quad (3)$$

and in the case of a charged particle with charge Z_1e, this force is

$$F = -\frac{(Z_1e)^2}{16\pi\sigma h^3}V, \quad (4)$$

where σ is the static conductivity. In the case where the particle moves perpendicular to the surface, an extra factor of 2 occurs in Eqs. (3) and (4). More general formulas describing damping of a dipole molecule and a charged particle were also derived in [4, 5]. No general formula has yet been derived for the damping force acting on a neutral atom moving perpendicular to the surface.

2. DAMPING FORCE ON THE MOVING NANOPROBE

We assume that the probe has the form of a paraboloid of revolution which is described by the canonical equation $z = d + (x^2 + y^2)/2R$, where z is measured from the surface of the sample, d is the minimum distance from the surface to the apex of the probe, and R is the probe's radius of curvature.

By using the Clausius–Mossotti equation, the atomic polarizability can be expressed in terms of the dielectric function $\varepsilon(\omega)$ of the material of the probe. Thus, we have

$$\alpha''(\omega) = \frac{3}{4\pi N}\mathrm{Im}\frac{\varepsilon(\omega) - 1}{\varepsilon(\omega) + 2}, \quad (5)$$

where N is the volume concentration of atoms. In what follows, the dielectric functions of the probe and the surface under investigation are labeled by indices 1 and 2, respectively. By substituting Eq. (5) into Eq. (1) and integrating over the probe's volume, the resultant lateral damping force can be found to be

$$F = -\frac{3}{64\pi}\frac{\hbar RV}{d^3}J(\varepsilon_1(\omega), \varepsilon_2(\omega)), \quad (6)$$

where $J(\varepsilon_1(w), \varepsilon_2(\omega))$ is the overlap integral of the spectra. The structure of this integral is identical to that of the integrand in Eq. (1), in which the imaginary part of the polarizability is replaced by the imaginary part of the quotient in Eq. (5) [4]. When deriving Eq. (6), it was also taken into account that, in the typical case, the AFM nanoprobe has a large aspect ratio (of height to radius of curvature) and, therefore, the upper limit of integration over the height of the probe can be extended to infinity. At $T = 0$, the numerical factor in Eq. (6) should be replaced by $3/32\pi$ and the integral $J(\varepsilon_1(\omega), \varepsilon_2(\omega))$ becomes identical to the integral in Eq. (2) with the substitution for the function $\alpha''(\omega)$ indicated above.

The dominating contribution to $J(\varepsilon_1(w), \varepsilon_2(\omega))$ comes from the frequency ranges where the absorption bands of the interacting solids strongly overlap. Therefore, the contributions from the different mechanisms operating in different spectral ranges should, in gen-

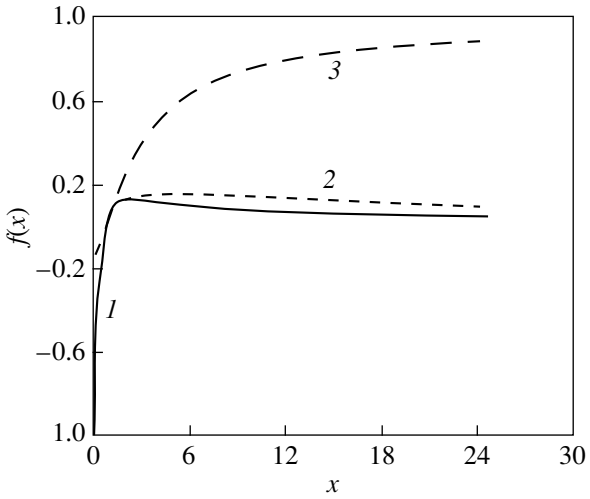

Fig. 1. Characteristic functions $f_1(x)$, $f_2(x)$, and $xf_1(x)$ (curves *1*, *2*, *3*, respectively). The ranges where these functions are negative correspond to nondissipative lateral forces.

eral, be taken into account. For uniform contacts, the functional $J(\varepsilon_1(\omega), \varepsilon_2(\omega))$ for some model dielectric functions was calculated numerically in our recent papers [4, 13]. However, analytical expressions for the friction forces are of prime interest. It turns out that closed expressions for these forces can be derived in the case where absorption in the low-frequency range of the electromagnetic spectra plays a dominant role.

First, we consider two conducting materials being in contact and represent the dielectric functions in the standard form:

$$\varepsilon_{1,2}(\omega) = 1 + i\frac{4\pi\sigma_{1,2}}{\omega}, \tag{7}$$

where $\sigma_{1,2}$ are the static conductivities. In order to take high-frequency spectral ranges into account, one should draw on formulas for the dynamical conductivities.

In the case of $\omega\hbar/2k_BT \ll 1$, where the temperature effects are significant, it is appropriate to use Eq. (1). By substituting Eqs. (5) and (7) into Eq. (1), the functional $J(\varepsilon_1(\omega), \varepsilon_2(\omega))$ can be represented in the form

$$J_1(a,b) = \int_0^\infty \frac{dx}{x}\left\{2\left[f_1(x)\frac{df_2(x)}{dx} - f_2(x)\frac{df_1(x)}{dx}\right] + x\left[f_1(x)\frac{d^2f_2(x)}{dx^2} - f_2(x)\frac{d^2f_1(x)}{dx^2}\right]\right\}, \tag{8}$$

where $f_1(x) = x/(x^2 + a^2)$ and $f_2(x) = x/(x^2 + b^2)$. All integrals in Eq. (8) are reduced to tabulated integrals, and, after complicated algebra, the function $J_1(a, b)$ is found to be

$$J_1(a,b) = \frac{\pi(b-a)}{ab(a+b)^2}. \tag{9}$$

At lower temperatures, where $\omega\hbar/2k_BT \gg 1$, Eq. (2) is more convenient to use, because the hyperbolic cotangent in Eq. (1) can be replaced by unity in this case. By substituting Eqs. (5) and (7) into Eq. (2) and performing integration, we obtain

$$J_2(a,b) = \int_0^\infty dx \frac{x}{x^2+a^2}\frac{d}{dx}\frac{x}{x^2+b^2} = \frac{(a^2+b^2)\ln(b/a) + (a^2-b^2)}{(a^2-b^2)^2}. \tag{10}$$

With these results, the damping force is written as

$$F = -\frac{9}{128\pi}\frac{k_BTRV}{d^3\sigma_1}f_1(x), \quad T \gg T_0, \tag{11a}$$

$$F = -\frac{3}{32\pi}\frac{\hbar RV}{d^3}f_2(x), \quad T \ll T_0, \tag{11b}$$

$$T_0 = \frac{\pi\hbar}{k_B}\max(2\sigma_1/3, \sigma_2), \quad x = 3\sigma_2/2\sigma_1, \tag{11c}$$

$$f_1(x) = \frac{x-1}{(1+x)^2}, \tag{12}$$

$$f_2(x) = \frac{(1-x^2+(1+x^2)\ln x)x}{(1+x^2)^2}. \tag{13}$$

Estimations show that $T_0 = 300$ K for $\max\sigma_{1,2} = 1400\ \Omega^{-1}\ \mathrm{m}^{-1}$; therefore, for materials (such as germanium and silicon) showing weak conductivity, smaller than the value indicated above, the temperature effects are significant and the damping force is proportional to the temperature and given by Eq. (11a). For metals, the parameter T_0 is very large and Eq. (11b) is valid in actual practice. Its singularity at $2\sigma_2 = 3\sigma_1$ is a seeming one; analysis shows that in this limit, we have $F = 0$, which is also the case for Eq. (11a) at $T = 0$. Thus, damping vanishes when the critical condition $2\sigma_2 = 3\sigma_1$ is fulfilled. At $2\sigma_2 < 3\sigma_1$, the lateral force on the nanoprobe becomes accelerative, because the probe gains energy from surface plasmons. The functions $f_1(x)$, $f_2(x)$, and $xf_1(x)$ [see Eq. (17a)], in terms of which the damping forces are calculated, are plotted in Fig. 1 (curves *1*, *2*, *3*).

An important feature of Eqs. (11) is their symmetry relative to interchanging the probe and the surface at $\sigma_1 = \sigma_2$. In this case, at $T = 0$, the damping force is quite independent of the conductivities and equals $F = -0.002\hbar RV/d^3$, which has a value of 0.0003 pN for typ-

ical AFM parameters $R = 30$ nm, $d = 0.3$ nm, and $V = 1$ m/s. At room temperature, for silicon–silicon-like tribometric contacts, more frequently used in AFM experiments, the damping force is much larger. For example, for $d = 0.3$ nm, $V = 1$ m/s, $R = 30$ nm, $T = 300$ K, and $\sigma = 0.001\ \Omega^{-1}\ \mathrm{m}^{-1}$, Eq. (11b) gives $F = 1$ nN, which is comparable to the adhesive friction force in the close-contact regime. We note that velocities of 0.06–6 m/s are typical of the dynamical mode of the AFM operation at an oscillation frequency of 1 MHz with amplitudes 10–1000 nm. It is possible that such (and even higher) velocities should also take place for the close-contact mode of the AFM operation in the initial short-run stage of the probe sliding over the surface.

Investigations of the interaction between two insulating materials and between a metal and an insulator are also of practical importance. A surface force apparatus [14] is commonly used to investigate insulator–insulator (e.g., mica–mica) interactions. We will approximate the dielectric functions of insulators in the low-frequency range by the Debye model expression:

$$\varepsilon(\omega) = 1 + \frac{\varepsilon - 1}{1 - i\omega\tau}, \tag{14}$$

where ε is the static permittivity and τ is the relaxation time (for mica, $\tau = 10^{-10}$–10^{-9} s). The approximations in Eq. (14) and Eq. (7) lead to the same functional of the dielectric functions. With Eqs. (9), (10), and (14), the damping forces for different combinations of materials can be written in the following unified form:

(1) For the insulating probe and the insulator surface,

$$F = -\frac{9k_B TRV\tau_1(\varepsilon_1 - 1)(\varepsilon_2 - 1)}{32d^3}\frac{}{(\varepsilon_1 + 2)^2(\varepsilon_2 + 1)} f_1(x), \quad T \gg T_0, \tag{15a}$$

$$F = -\frac{3}{32\pi}\frac{\hbar RV}{d^3}\frac{(\varepsilon_1 - 1)(\varepsilon_2 - 1)}{(\varepsilon_1 + 2)(\varepsilon_2 + 1)} f_2(x), \quad T \ll T_0, \tag{15b}$$

$$T_0 = \frac{2\hbar}{k_B}\max((\varepsilon_1 + 2)/3\tau_1;\ (\varepsilon_2 + 1)/2\tau_2), \qquad x = 3\tau_1(\varepsilon_2 + 1)/2\tau_2(\varepsilon_1 + 2); \tag{15c}$$

(2) For the conducting probe and the insulator surface,

$$F = -\frac{9}{128\pi}\frac{k_B TRV}{d^3}\frac{(\varepsilon - 1)}{\sigma(\varepsilon + 1)} f_1(x), \quad T \gg T_0, \tag{16a}$$

$$F = -\frac{3}{32\pi}\frac{\hbar RV}{d^3}\frac{(\varepsilon - 1)}{(\varepsilon + 1)} f_2(x), \quad T \ll T_0, \tag{16b}$$

$$T_0 = \frac{2\hbar}{k_B}\max(4\pi\sigma/3, (\varepsilon + 1)/2\tau), \qquad x = \frac{3(\varepsilon + 1)}{8\pi\sigma\tau}; \tag{16c}$$

(3) For the insulating probe and the conductor surface,

$$F = -\frac{9}{64\pi}\frac{k_B TRV}{d^3}\frac{(\varepsilon - 1)}{(\varepsilon + 2)\sigma} f_1(x)x, \quad T \gg T_0, \tag{17a}$$

$$F = -\frac{3}{32\pi}\frac{\hbar RV}{d^3}\frac{(\varepsilon - 1)}{(\varepsilon + 2)} f_2(x), \quad T \ll T_0, \tag{17b}$$

$$T_0 = \frac{\hbar}{2k_B}\max\left(\frac{\varepsilon + 2}{3\tau}, 2\pi\sigma\right), \quad x = \frac{6\pi\sigma\tau}{\varepsilon + 2}. \tag{17c}$$

For silicon–mica contacts, we have $T_0 < 0.1$ K and, therefore, Eqs. (15a), (16a), and (17a) are valid under any typical experimental conditions. As seen from Fig. 1, the sign of the lateral force can be different, depending on the ratio between the conductivities, the ratio between the relaxation times, or the product $\sigma\tau$.

It should be stressed once again that the formulas derived in this paper determine only that part of the fluctuational electromagnetic force which is due to absorption in the low-frequency spectral range. Additional contributions can arise if the absorption bands overlap in other spectral ranges.

3. A COMPARISON WITH AFM DATA

It is of considerable interest to compare the theoretically calculated fluctuational dissipative forces with the available experimental AFM data. In [2], the dissipative forces were measured experimentally in the case where the AFM silicon probe moved along a normal to the surface of mica in a vacuum. The cantilever had stiffness $k = 40$ N/m and natural frequency $f = 300$ MHz, and the radius of curvature of the probe was $R = 20$ nm. For an amplitude of $A = 20$ nm, the energy loss per cycle was measured to be $\Delta W = 1$–10 eV, depending on the ratio d/A, where d is the initial spacing between the probe apex and the surface in the absence of oscillations. In this case, the quality factor of the oscillating probe $Q = \pi kA^2/\Delta W$ equals $(0.3$–$3.0) \times 10^5$. It is obvious that, for lateral oscillations of the probe at the same frequency and the same (fixed) spacing between the probe apex and the surface, equal to $h = d - A$, the energy loss rate is somewhat higher and the quality factor is lower.

By representing Eq. (16a) in the form $F = -\gamma RTV/h^3$, the theoretical quality factor associated with fluctuational forces is found to be $Q_t = kh^3/4\pi f\gamma RT$. For $\varepsilon = 6$, $\tau = 10^{-9}$ s, and $\sigma = 0.001\ \Omega^{-1}\ \mathrm{m}^{-1}$, we obtain from Eqs. (16a)–(16c) that $\gamma \approx 0.019k_B\tau$. For the same values of the probe parameters and $h = 0.3$ nm, the quality factor is equal to $Q_t = 5.3 \times 10^7/T$. Therefore, at temperatures 100–300 K, Q_t is of the same order of magnitude as the experimental values [2].

It should be noted that, in the case considered above, Q_t virtually does not depend on the conductivity of the probe, but decreases in inverse proportion to increasing relaxation time of the dielectric. On the whole, we have

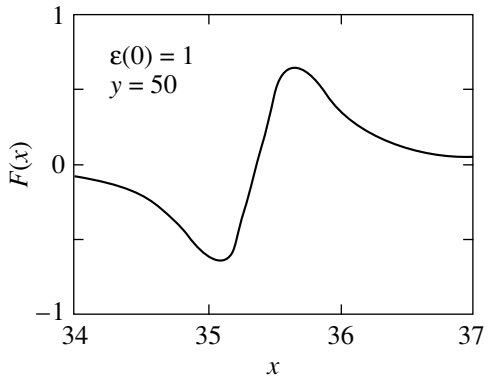

Fig. 2. Function $F(x)$ given by Eq. (21) ($x_i \equiv x$).

$Q_t \propto kh^3/f\tau RT$ in this case; this permits verification of the predictions of the theory, which enables one to measure fluctuational electromagnetic forces. As has already been noted above, a surprising prediction of the theory is that the lateral damping force acting on the probe can vanish and even become positive (Fig. 1). In the case of the silicon–mica contact, the damping force vanishes at $\sigma = 3(\varepsilon + 1)/8\pi\tau$; therefore, for a fixed value of τ, this condition can easily be satisfied by choosing the appropriate doped material for the probe.

In the experiment under discussion, the energy loss can be associated not only with fluctuational dissipative forces, but also with the breaking of adhesion bonds, although the latter mechanism is more typical of the close-contact mode of the AFM operation [1]. However, the damping force due to the breaking of adhesion bonds is independent of the velocity and electrophysical properties and is likely to depend on the temperature only slightly [13]. These specific features can help in the separation of the corresponding contributions to the damping force.

4. FLUCTUATIONAL DISSIPATIVE FORCES AND QUARTZ-MICROBALANCE MEASUREMENTS

Fluctuational dissipative forces can also be determined from crystalline-quartz microbalance experiments [6, 7], in which one measures the oscillation damping of quartz oscillators (metal-coated quartz plates). The presence of a film of adsorbed inert gases on the surface of the plate causes a change in the Q factor of the oscillator and allows one to estimate the characteristic decay time of the translational motion of adsorbed atoms. In the case of krypton on the surface of gold, this time is about 1 ns.

Let us estimate the decay time due to fluctuational electromagnetic forces from Eq. (2). The imaginary part of the atomic polarizability can be written in the most general case as (e and m are the charge and mass of an electron, respectively)

$$\alpha''(\omega) = \frac{e^2}{m}\sum_i \frac{f_i\gamma_i\omega}{(\omega_i^2 - \omega^2)^2 + \gamma_i^2\omega^2}, \qquad (18)$$

where the sum is over all electron transitions from the ground state (0) of the atom to the excited states (i) of the discrete spectrum and ω_i, γ_i, and f_i are the transition frequency, linewidth, and oscillator strength, respectively. The high-frequency dielectric function of the metal or semiconductor coating of the plate can be written in the standard Drude approximation as ($\varepsilon = 1$ for the metal coating)

$$\varepsilon(\omega) = \varepsilon - \frac{(\omega_p\tau)^2}{1 + (\omega\tau)^2} + \frac{i(\omega_p\tau)^2}{\omega\tau(1 + (\omega\tau)^2)}, \qquad (19)$$

where ω_p is the plasma frequency and τ is the relaxation time for electrons.

By substituting Eqs. (18) and (19) into Eq. (2) and going to the limit $\gamma_i \longrightarrow 0$, we obtain

$$F = \frac{3\hbar e^2\tau^2 V}{4mz^5}\Phi(a, y), \qquad (20)$$

$$\Phi(a, y) = \sum_i \frac{f_i y^2(3a^2x_i^4 - 2ax_i^2y^2 + a^2x_i^2 - y^4)}{x_i(a^2x_i^4 - 2ax_i^2y^2 + a^2x_i^2 + y^4)^2} = \sum_i F_i(a, y, x_i) f_i y^2, \qquad (21)$$

where $a = \varepsilon + 1$, $x_i = \omega_i\tau$, and $y = \omega_p\tau$.

Analysis shows that the terms in the sum in Eq. (21) can have any sign. For metals, we have $y \gg 1$ and the $F_i(a, y, x_i)$ vanish at $\sqrt{2}\,w_i \approx w_p$ for fixed values of x_i. The contributions from the transition frequencies $w_i \geq w_p/\sqrt{2}$ correspond to an accelerative force; the other frequencies contribute to the damping force. In order to compute the function $\Phi(a, y)$, the specific distribution of oscillator strengths should be given.

Figure 2 shows the dependence of $F_i(a, y, x_i)$ on x_i for the parameter values typical of gold: $\omega_p = 8.8$ eV, $\tau = 3.7 \times 10^{-15}$ s, $a = 2$, $y = 50.2$, and $f_i \equiv 1$. It is seen from Fig. 2 that $F_i(a, y, x_i)$ has no singularities, because $x_i > 0$; however, this function exhibits a characteristic nonmonotonic change in the narrow spectral range around $x_i \approx y/\sqrt{2}$, and, therefore, the dominant contribution to $\tilde{\Phi}(a, y)$ comes from these transition frequencies. By putting $f_i \approx 0.1$ and $df/dx \propto x^{-3.5}$ (which adequately describes the optical and UV ranges of the spectrum) and converting the sum in Eq. (21) to an integral, we arrive at the function $\tilde{\Phi}(a, y)$ plotted in Fig. 3. It is seen that, where the lateral force is negative,

$\tilde{\Phi}(a, y) < 0$, which corresponds to the case of usual damping.

For the surface of gold, we have $\tilde{\Phi}(2, 50.2) = -0.093$. Using this result and Eq. (20), for the case of a Kr atom adsorbed at a distance of 0.4 nm from the surface, we obtain the decay time $\Delta t = MV/F \approx 0.6$ ns (M is the mass of a Kr atom), which is close to the experimental value. It should be noted, however, that the value of Δt is very sensitive to variations in τ, ω_p, and z, as is seen from Eqs. (20) and (21) and Fig. 3.

If adsorbed atoms form a film, an additional contribution to the damping force can arise because of absorption in the low-frequency spectral range. Another factor leading to an increase in the damping force can be the appearance of localized dipole moments and electric charges on adsorbed atoms. The corresponding damping forces are given by Eqs. (3) and (4), and these are fairly small in the case of good conductors, such as gold. For example, for $Z_1 = 1$, the dipole moment $d = 1$D and $z = 0.4$ nm, the damping forces are 4–5 orders of magnitude smaller than those given by Eq. (20) and can be ignored. A completely different type of situation can occur for the surface of graphite and silicon.

5. THE INTERACTION BETWEEN PLANE SURFACES

The fluctuational dissipative forces per unit area of the interacting surfaces were recently calculated [8–10] using the Maxwell stress tensor for the case where two parallel thick plates divided by a gap of width d move relative to each other. An extended discussion of those calculations is beyond the scope of this paper. However, it should be noted that there is a fundamental discrepancy concerning the finite damping force proportional to the velocity at $T = 0$; in contrast to our paper, this force is missing from the results of the papers mentioned.

It is our opinion that the electric field in the gap was calculated incorrectly in [8–10]. For example, Pendry [8] used a heuristic expression for the field amplitude, which allows for the inherent fluctuating field of one of the plates and the field of the wave reflected from the other plate, with the Fresnel reflection coefficient including the Doppler shift due to the relative motion of the surfaces. Volokitin and Persson [9, 10] used a more general method, but their dynamical generalization of formulas of the Lifshitz fluctuation theory for the electromagnetic field amplitude is not evident and, furthermore, a number of additional approximations were made when passing over from the original relativistic theory to the nonrelativistic case. The expressions derived in [9, 10] for the damping force at $T = 0$ are identical to those obtained by Pendry; however, at $T \neq 0$, the contribution to the damping force proportional to the velocity is quadratic in T.

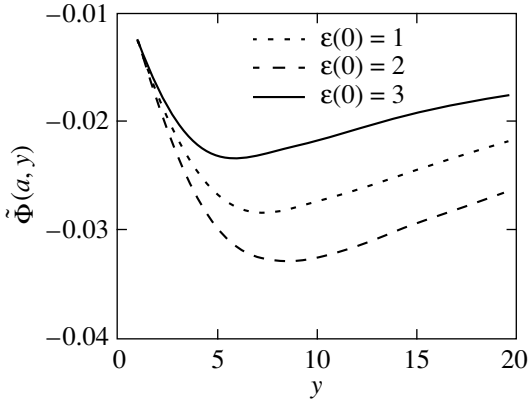

Fig. 3. Function $\tilde{\Phi}(a, y)$.

In order to go to the case of two interacting plates in our formulas for the damping force exerted on the convex probe by the plane surface, it is sufficient, rather than to integrate over the probe volume, to integrate Eq. (1) or Eq. (2) over h (from zero to infinity) and divide the result by the area S of the surface of the plate. Then, e.g., instead of Eq. (6), one obtains

$$\frac{F}{S} = -\frac{9\hbar V}{128\pi^2 d^4} J(\varepsilon_1(\omega), \varepsilon_2(\omega)). \qquad (22)$$

The friction stress F/S for different combinations of materials is obtained by multiplying the right-hand sides of Eqs. (11) and (15)–(17) by a factor of $3/2\pi Rd$. Thus, in the case under discussion, the dependence on the gap width follows a power law with an exponent (in the denominator) larger by unity than that in the case of an interaction between the parabolic probe and the plane surface.

We note that a formula little different from Eq. (22) is derived from an intermediate result obtained by Pendry (Eq. (18) in [8] in the low-velocity limit). In comparison with Eq. (22), this formula has an extra factor 4/9 and, in the spectrum-overlap integral analogous to the integral in Eq. (2), $\alpha''(\omega)$ is replaced by $\mathrm{Im}[(\varepsilon_1(\omega) - 1)/(\varepsilon_1(\omega) + 1)]$. It is clear that the factor 4/9 appears because the contribution from the other plate is not taken into account. However, the original expression is not symmetric under the permutation of indices $1 \longleftrightarrow 2$ and its formal symmetrization, performed in [8], resulted in a final symmetric expression in which the contributions to the damping force linear in velocity canceled each other out. Furthermore, even without symmetrization, the damping force also becomes zero for plates of the same type, in contrast to Eq. (22). This shows once again that the approximation made in [8] suffers from shortcomings. For the purposes of this paper, however, the most important point is that although the results obtained in [8–10] are based on the continuum model and do not involve the assumption that the interactions are additive, these results lead to

the same dependence of the damping force on the distance d as that in Eq. (22).

In actual practice, the calculations of the fluctuational forces acting between plane surfaces are of importance in surface-force apparatus experiments [14], in which one measures the friction forces between mica plates covered with surfactants.

6. CONCLUSIONS

Thus, the theoretical model proposed in [4, 5] for calculating nonrelativistic dynamical fluctuational dissipative forces is developed further. We derived closed analytical formulas for the damping forces acting between a parabolic nanoprobe and a plane surface, between a neutral spherical atom and a conducting surface, and between parallel thick plates divided by a gap. The metal–metal, insulator–insulator, metal–insulator, and insulator–metal contacts are considered. The formulas derived allow for absorption of electromagnetic waves in the low-frequency spectral range and predict characteristic dependences of the damping forces upon velocity, temperature, distance, nanoprobe radius, and electrical characteristics of interacting solids. In particular, it is predicted that, in all cases considered in this paper, the damping force proportional to the velocity does not vanish at zero temperature. The conditions for nondissipative slide of surfaces are discussed.

The Q factor of oscillators is estimated for the modulation mode of the AFM operation, and a comparison with the experimental data is made for the case of a silicon nanoprobe interacting with mica. The calculated and experimental fluctuational electromagnetic forces are shown to be of the same order of magnitude (0.001–1 nN), so that their AFM measurement is feasible.

It is also shown that the damping time for moving adatoms measured in quartz microbalance experiments can be associated with fluctuational electromagnetic forces.

REFERENCES

1. G. V. Dedkov, Usp. Fiz. Nauk **170** (6), 585 (2000); Phys. Status Solidi A **179** (1), 2 (2000).
2. B. Gotsmann, C. Seidel, B. Anczykowski, and H. Fuchs, Phys. Rev. B **60** (15), 11051 (1999).
3. I. Dorofeyev, H. Fuchs, G. Wenning, and B. Gotsmann, Phys. Rev. Lett. **83** (12), 2402 (1999).
4. G. V. Dedkov and A. A. Kyasov, Phys. Lett. A **259**, 38 (1999); Pis'ma Zh. Tekh. Fiz. **25** (12), 10 (1999) [Tech. Phys. Lett. **25**, 466 (1999)].
5. G. V. Dedkov and A. A. Kyasov, Fiz. Tverd. Tela (St. Petersburg) **43** (1), 169 (2001) [Phys. Solid State **43**, 176 (2001)]; Surf. Sci. (2000).
6. E. T. Watts, J. Krim, and A. Widom, Phys. Rev. B **41** (6), 3466 (1990).
7. J. Krim, D. H. Solina, and R. Chiarello, Phys. Rev. Lett. **66** (2), 181 (1991).
8. J. B. Pendry, J. Phys. C **9** (8), 10301 (1997).
9. A. I. Volokitin and B. N. J. Persson, Phys. Low-Dimens. Semicond. Struct. **7** (8), 1 (1998).
10. A. I. Volokitin and B. N. J. Persson, J. Phys.: Condens. Matter **11** (2), 345 (1999).
11. P. Johansson and P. Apell, Phys. Rev. B **56** (7), 4159 (1997).
12. Yu. N. Moiseev, V. M. Mostepanenko, and V. I. Panov, Phys. Lett. A **132** (6–7), 354 (1988).
13. G. V. Dedkov, Mater. Lett. **38** (5), 360 (1999); Wear **232** (2), 145 (1999).
14. J. N. Israelachvili, *Intermolecular and Surface Forces* (Academic, New York, 1992).

Translated by Yu. Epifanov